ELSEVIER Journal of Materials Processing Technology 53 (1995) 798–810

Journal of Materials Processing Technology

# A mechanics model for sheet-metal stamping using deformable dies

L.C. Zhang

*Department of Mechanical and Mechatronic Engineering, The University of Sydney, NSW 2006, Australia*

Received 22 April 1994

**Industrial Summary**

This paper studied the deformation mechanisms of sheet metals stamped by rigid punches and deformable dies. Emphasis was placed on the development of elastic–plastic zones in the sheet workpieces, on the functions of the die parameters and on their correlations with spring-back. It was found that the reduction of spring-back was due mainly to the interface interaction offered by the dies. The paper provides new insight into processing techniques subjected to plane-strain conditions.

## Nomenclature

| | |
|---|---|
| $a$ | half contact-length between the plate and the punch, see Fig. 1 and Eq. (19) |
| $b$ | width of the plate |
| $c$ | half-width of the elastic stress/strain distribution on a plate section, see Figs. 5 and 6 |
| $d$ | distance between the mid-plane and the neutral stress/strain plane of the plate, see also Figs. 5 and 6 |
| $E$ | Young's modulus of the plate material |
| $E_f$ | Young's modulus of the elastic foundation |
| $E_p$ | plastic hardening modulus of the plate material, see also Fig. 4 |
| $e$ | non-dimensional parameter, defined as $E_p/E$ |
| $h$ | thickness of the plate |
| $k$ | spring constant, see Fig. 3 |
| $L$ | half-length of the plate in contact with the die, see Figs. 1–3 |
| $M$ | bending moment on a plate section |
| $M_e$ | maximum elastic bending moment, defined by Eq. (3) |
| $m$ | non-dimensional bending moment, see Eq. (2) |
| $N$ | axial force on a plate section |
| $N_e$ | maximum elastic axial force, defined by Eq. (3) |


*SSDI* 0924-0136(94)01765-S

| | |
|---|---|
| $n$ | non-dimensional axial force, defined by Eq. (2) |
| $p(x)$ | normal force on the plate surface, see Fig. 2 |
| $q(x)$ | tangential force on the plate surface, see Fig. 2 |
| $u$ | horizontal displacement at the end of the plate, see Fig. 3 |
| $w$ | deflection of the plate |
| $x$ | horizontal coordinate |
| $\gamma, \delta$ | non-dimensional parameters, defined by Eq. (4) |
| $\varepsilon$ | strain |
| $\varepsilon_Y$ | yield strain, $= \sigma_Y/E$ |
| $\zeta$ | non-dimensional coordinate, defined as $x/L$ |
| $\eta$ | non-dimensional deflection, defined as $w/(L^2\kappa_e)$ |
| $\Theta$ | the springback ratio, defined by Eq. (13) |
| $\kappa$ | curvature at $x$ |
| $\kappa_e$ | maximum elastic curvature at $x$ |
| $\mu$ | proportional function for interface friction, defined by Eq. (1) |
| $v$ | Poisson's ratio of the plate material |
| $v_f$ | Poisson's ratio of the elastic foundation |
| $\xi$ | material parameter, see Fig. 4 |
| $\sigma_Y$ | yield stress of the plate material, see Fig. 4 |
| $\phi$ | non-dimensional curvature, defined by Eq. (2) |
| $\phi^R$ | non-dimensional residual curvature, defined as $\kappa^R/\kappa_e$ |

Superscripts

| | |
|---|---|
| c | central section, i.e., the plate section at $x = 0$ |
| U | upper surface of the plate |
| L | lower surface of the plate |

## 1. Introduction

The technique of elastic–plastic sheet stamping has been employed extensively in the forming of a variety of engineering components. In addition to the conventional processes, with unitary rigid dies, a technique of sheet stamping by deformable forming tools (SSDFT) has been established and designed into a wide range of pressworking [1]. Compared with conventional process, SSDFT possesses the distinct advantages of low tooling costs, flexibility of producible shapes, the capability for providing "scratch-free" surfaces which is most suitable for parts with coated or polished surfaces, and a remarkable reduction of spring-back and wrinkling which is extremely important for hard-to-forming sheet materials. Unfortunately, the process has not been studied carefully so that proper guidelines are not available for practical manufacturing design.

The present paper aims to investigate, with the aid of mechanics modelling, the deformation mechanisms of sheet metals stamped by rigid punches and deformable dies. The development of elastic–plastic zones in the sheet workpieces, the functions of die parameters and their correlations with spring-back are addressed in detail.

The study reveals that the reduction of spring–back is due mainly to the interface interaction offered by the dies. The paper provides new insight into processing techniques subjected to plane-strain conditions.

## 2. Problem characterisation

### 2.1. Stamping of wide plates by deformable dies

Consider a wide thin plate resting on a deformable die stamped by a rigid cylindrical punch, see Fig. 1. The deformation of the plate is symmetrical and the bending is cylindrical. On the upper surface of the plate, there are a normal contact force $p^{\mathrm{U}}(x)$ and a tangential force $q^{\mathrm{U}}(x)$ distributed over a small contact arc, $AA'$. On the lower surface, the corresponding forces are $p^{\mathrm{L}}(x)$ and $q^{\mathrm{L}}(x)$, respectively, see Fig. 2, exerted on the contact length, $2L$, which is less than the whole length of the plate because of the existence of lifted parts at the ends. Owing to the symmetry of deformation, $p^{\mathrm{U}}(x)$ and $p^{\mathrm{L}}(x)$ must be symmetrical but $q^{\mathrm{U}}(x)$ and $q^{\mathrm{L}}(x)$ anti-symmetrical, with respect to $x$.

### 2.2. Mechanics modelling

To explore clearly the deformation mechanism of the plate, it is essential to distil a mechanics model for the above engineering process, that can reflect the main characteristics of the original but also can simplify the problem to a great extent such that an analytical solution can be generated.[1]

It is reasonable to assume, by noting the small plate thickness, that $q^{\mathrm{U}}(x)$ and $q^{\mathrm{L}}(x)$ contribute to the total axial force $N(x)$ only, whilst $p^{\mathrm{U}}(x)$ and $p^{\mathrm{L}}(x)$ contribute to the bending moment $M(x)$ only. The mechanics model is shown in Fig. 3. A thin plate of thickness $h$, width $b$ and length $2L$ ($h \ll 2L$) subjected to a set of transverse loads (distributed uniformly along the width $b$) is simply supported but with variable axial restraints (springs) at the two ends. The springs provide a uniform axial force (as a function of the plate deflection to simulate possible external tension). Another part of $N$ is assumed to be proportional to $p^{\mathrm{L}}(x)$ to represent the friction on the interface. Consequently:

$$N(x) = b \int_x^L \mu(\xi) p^{\mathrm{L}}(\xi)\,\mathrm{d}\xi + ku, \tag{1}$$

where $\mu(x)$ is a proportional function, $k$ is the stiffness of the springs and $u$ is the horizontal displacement at the plate ends (Fig. 3).

---

[1] Although numerical methods such as the finite-element and finite-difference methods could be applied to take into account more details, they cannot replace a modelling approach that reveals thoroughly the deformation mechanisms.

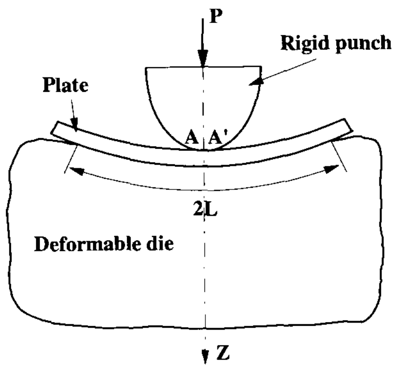


Fig. 1. Stamping by a deformable die.

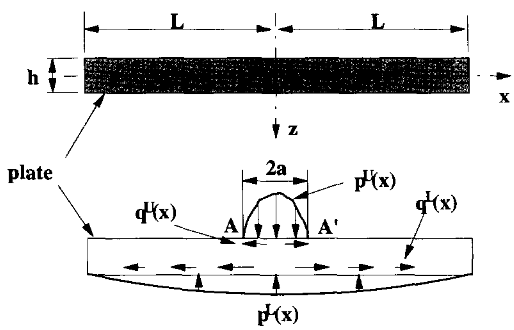


Fig. 2. Interface forces on the plate.

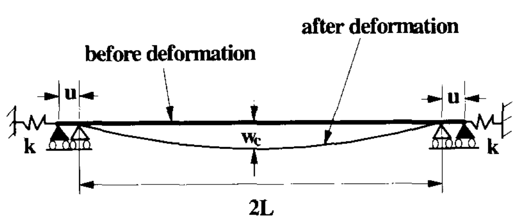


Fig. 3. A mechanics model for plate stamping.

## 3. Analysis

### *3.1. Load–curvature relationships*

A complete relationship between internal loads and deformation at any plate section should be established first. The uniaxial stress–strain behaviour of most sheet

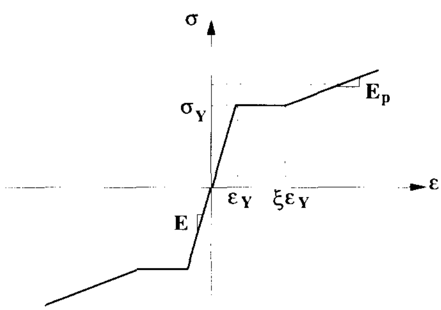


Fig. 4. The stress strain curve of the plate material.

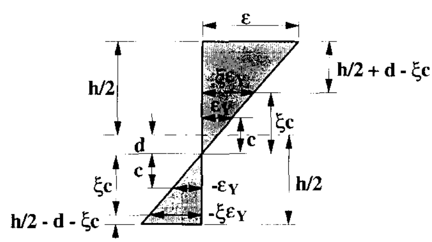


Fig. 5. Strain distribution across the plate thickness.

metals can be characterised by the model shown in Fig. 4. When the length of the yield platform approaches zero (i.e., $\xi \rightarrow 0$), it represents an elastic–linearly plastic hardening material, but when the hardening modulus $E_p$ is zero, it becomes an elastic–perfectly plastic model. Assuming that plane sections of the plate remain plane throughout the deformation, the strain across the plate thickness is then always linear, see Fig. 5. Correspondingly, the stress distribution across a plate section at coordinate $x$ under different combinations of $M$ and $N$ must be one of the following six types (see Fig. 6):[2] (i) the pure elastic state (S1); (ii) the single-side perfectly plastic state (S2); (iii) the double-side perfectly plastic state (S3(a)); (iv) the single-side hardening plastic state with the other side being elastic (S3(b)); (v) the single-side hardening plastic state with the other side being perfectly plastic (S4); and (vi) the double-side hardening plastic state (S5).

The non-dimensional bending moment, axial force and curvature, are defined as follows:

$$m = \frac{M}{M_e}, \qquad n = \frac{N}{N_e}, \qquad \phi = \frac{\kappa}{\kappa_e}, \tag{2}$$

[2] In the description of Figs. 5 and 6 it has been assumed that the neutral strain and neutral stress layers are identical: refined theories can be found in [1].

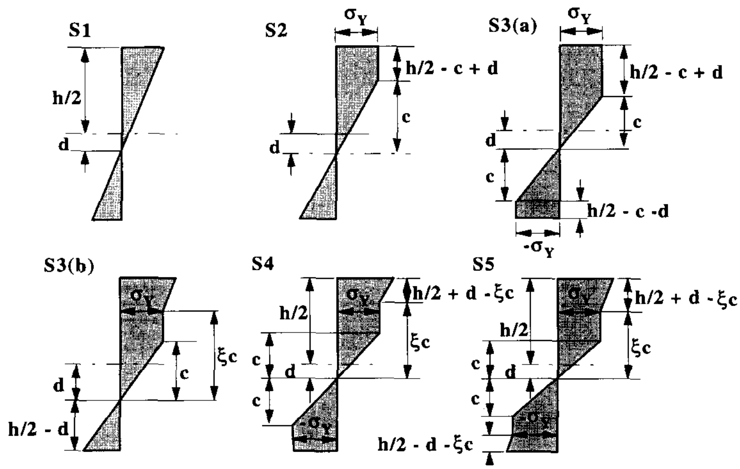


Fig. 6. Possible stress states in the plate.

where

$$M_e = \frac{1}{6}\sigma_Y bh^2, \qquad N_e = \sigma_Y bh, \qquad \kappa_e = \frac{2\sigma_Y}{hE} \tag{3}$$

are the maximum elastic bending moment; the maximum elastic axial force; and the maximum elastic curvature; respectively, in which $\sigma_Y$ is the yield stress and $E$ is Young's modulus. Furthermore, the non-dimensional parameters

$$\gamma = \frac{c}{(h/2)}, \qquad \delta = \frac{d}{(h/2)} \tag{4}$$

are introduced throughout the analysis ($c$ and $d$ are shown in Figs. 5 & 6). The load–curvature relationships for the above six states and their corresponding boundary conditions can be obtained from Figs. 5 & 6 directly:

(S1) $1 + \delta - \gamma \leqslant 0$:

$$n = \frac{\delta}{\gamma}, \qquad m = \frac{1}{\gamma}, \qquad \phi = m. \tag{5}$$

(S2) $1 + \delta - \gamma \geqslant 0$ and $1 - \delta - \gamma \leqslant 0$:

$$n = 1 - \frac{1}{4\gamma}(1 - \delta + \gamma)^2,$$

$$m = \frac{1}{4\gamma}(1 - \delta + \gamma)^2[3 - (1 - \delta + \gamma)], \tag{6}$$

$$\phi = 4(1 - n)\Big/\left(3 - \frac{m}{1 - n}\right)^2.$$

There are two possibilities for the further development of the present stress state, relying on the parameter of the material property, $\xi$. For example, if $\xi$ is relatively large the stress state will evolve into (S3(a)), otherwise if it is very close to unity the following state will be (S3(b)).

(S3(a)) $1 - \delta - \gamma \geqslant 0$ and $1 + \delta - \xi\gamma \leqslant 0$:

$$n = \delta, \qquad m = \tfrac{3}{2}(1 - \delta^2) - \tfrac{1}{2}\gamma^2, \qquad \phi = [3(1 - n^2) - 2m]^{-1/2} \tag{7}$$

(S3(b)) $1 - \delta - \gamma \leqslant 0$ and $1 + \delta - \xi\gamma \geqslant 0$:

$$n = 1 - \frac{1}{4\gamma}(1 - \delta + \gamma)^2 + \frac{e}{4\gamma}(1 + \delta - \xi\gamma)^2,$$

$$m = \frac{1}{4\gamma}(1 - \delta + \gamma)^2[3 - (1 - \delta + \gamma)] + \frac{e}{4\gamma}(1 + \delta - \xi\gamma)^2[3 - (1 + \delta - \xi\gamma)], \tag{8}$$

where $e = E_p/E$. According to Eq. (8a):

$$\delta = (1 - e)^{-1}\left\{1 + e + (1 - e\xi)\gamma - \sqrt{e\left[(\xi - 1)^2\gamma^2 + 4\left(n - \xi - \frac{n-1}{e}\right)\gamma + 4\right]}\right\}. \tag{9}$$

The load-curvature relationship can be obtained explicitly if Eq. (9) is substituted into Eq. (8b) and $\gamma$ is replaced by $\phi^{-1}$. Particularly, if $e$ approaches zero, $\delta$ in Eq. (9) will becomes that of (S2). Any further development of stress state from either (S3(a)) or (S3(b)) will lead to (S4).

(S4) $1 + \delta - \xi\gamma \geqslant 0$, $1 - \delta - \gamma \geqslant 0$ and $1 - \delta - \xi\gamma \leqslant 0$:

$$\begin{aligned} n &= \delta + \frac{e}{4\gamma}(1 + \delta - \xi\gamma)^2, \\ m &= \frac{3}{2}(1 - \delta^2) - \frac{1}{2}\gamma^2 + \frac{e}{4\gamma}(1 + \delta - \xi\gamma)^2[3 - (1 + \delta - \xi\gamma)]. \end{aligned} \tag{10}$$

An explicit load–curvature relationship can be derived when $\gamma = \phi^{-1}$ and

$$\delta = \{2\sqrt{\gamma[\gamma + e(1 - \xi\gamma + n)]} - e(1 - \xi\gamma) - 2\gamma\}/e \tag{11}$$

are substituted into Eq. (10b). Similarly, Eq. (11) will be identical to that of (S3(a)) when $e$ approaches zero.

(S5) $1 - \delta - \xi\gamma \geqslant 0$:

$$\begin{aligned} n &= \left[1 + \frac{e}{\gamma}(1 - \xi\gamma)\right]\delta, \\ m &= \frac{3}{2}(1 - \delta^2) - \frac{1}{2}\gamma^2 + \frac{e}{2\gamma}[(1 - \xi\gamma)^2(2 + \xi\gamma) + 3\xi\gamma\delta^2]. \end{aligned} \tag{12}$$

The combination of Eqs. (12a) and (12b) gives rise to the load-curvature relationship straight-forwardly.

There are two special cases, $\xi = 1$ ($e \neq 0$) and $e = 0$. In the former, only regimes (S1), (S3(b)) and (S5) will appear, but in the latter only (S1), (S2) and (S3(a)) will occur, which is the case studied by Yu and Johnson [2].

### 3.2. Spring–back ratio

If the unloading process is totally elastic, the spring–back ratio of a plate section, $\Theta$, is given by:

$$\Theta \equiv (\phi - \phi^{\mathrm{R}})/\phi = m/\phi \tag{13}$$

when the bending moment and axial force have been removed, where $\phi^{\mathrm{R}} = \kappa^{\mathrm{R}}/\kappa_{\mathrm{e}} = \phi - m$ is the non-dimensional residual curvature of the plate. Accordingly, with $\phi$ and $m$ determined by Eqs. (5)–(12), $\Theta$ can be predicted very easily from Eq. (13).

### 3.3. Deflection curve

Because of the symmetry of deformation, only half of the plate, say $0 \leqslant x \leqslant L$, needs to be analysed, see Figs. 1–3. The deflection curve of the plate is determined by integrating the deflection–curvature equation:

$$\frac{\mathrm{d}^2 w}{\mathrm{d}x^2} - \kappa(x)\left[1 + \left(\frac{\mathrm{d}w}{\mathrm{d}x}\right)^2\right]^{3/2} = 0. \tag{14}$$

When $w$ is small compared with $L$, Eq. (14) can be simplified to:

$$\frac{\mathrm{d}^2 w}{dx} - \kappa(x) = 0. \tag{15}$$

Introducing the non-dimensional deflection $\eta$ and coordinate $\zeta$, i.e.:

$$\eta = \frac{w}{L^2\kappa_{\mathrm{e}}} = \frac{whE}{2L^2\sigma_{\mathrm{Y}}}, \qquad \zeta = \frac{x}{L}, \tag{16}$$

Eq. (15) becomes

$$\frac{\mathrm{d}^2\eta}{\mathrm{d}\zeta^2} - \phi = 0. \tag{17}$$

The boundary conditions in the present case are:

$$\eta\bigg|_{\zeta=1} = 0, \qquad \frac{\mathrm{d}\eta}{\mathrm{d}\zeta}\bigg|_{\zeta=0} = 0. \tag{18}$$

### 3.4. Solution procedure

The detailed explicit expressions derived above enable solutions to be obtained easily. The following procedures are used for the numerical calculations in the present paper:

(i) determine $n$ with the value of $\eta_c^*$ given;
(ii) compute $m(\zeta)$ according to the given loads $p^U$ and $p^L$;
(iii) calculate $\phi(\zeta)$;
(iv) integrate Eq. (17) to obtain $\eta(\zeta)$ under the conditions specified by Eq. (18);
(v) if $\eta_c \approx \eta_c^*$, calculate $\Theta$ and stop, otherwise, continue;
(vi) let $\eta_c^* = \eta_c$ and return to step (i).

## 4. Discussion

To obtain a detailed diagram for the correlation of the deformation of the plate and the die, a convenient and natural starting point is to assume that both $p^L(x)$ and $p^U(x)$ are Hertzian, i.e.:

$$p^U(x) = \bar{p}^U\left(1 - \frac{x^2}{a^2}\right)^{1/2}, \qquad p^L(x) = \bar{p}^L\left(1 - \frac{x^2}{L^2}\right)^{1/2}, \tag{19}$$

where $a$ is the half length of the contact arc $AA'$ between the punch and plate, see Fig. 1, and $\bar{p}^L$ and $\bar{p}^U$ are the maximum pressure values of $p^L(x)$ and $p^U(x)$ at $x = 0$ related by force equilibrium in the $z$-direction (it is assumed that the springs do not contribute in this direction). This gives rise to $\bar{p}^L = a\bar{p}^U/L$. The bending moment in the plate is therefore:

$$\begin{aligned} m(\zeta) &= \frac{aL\bar{p}^U}{h^2\sigma_Y}\left\{2\left[\sqrt{(1-\zeta^2)^3} - \zeta_a\sqrt{\left(1-\frac{\zeta^2}{\zeta_a^2}\right)^3}\,\right]\right. \\ &\quad + 3\zeta\left(\left[\zeta\sqrt{1-\zeta^2} + \arcsin\zeta - \frac{\pi}{2}\right]\right. \\ &\quad \left.\left. - \left[\frac{\zeta}{\zeta_a}\sqrt{1-\frac{\zeta^2}{\zeta_a^2}} + \arcsin\frac{\zeta}{\zeta_a} - \frac{\pi}{2}\right]\right)\right\} \\ &\quad \text{for } 0 \leqslant \zeta \leqslant \zeta_a, \\ m(\zeta) &= \frac{aL\bar{p}^U}{h^2\sigma_Y}\left\{2\sqrt{(1-\zeta^2)^3} + 3\zeta\left[\zeta\sqrt{1-\zeta^2} + \arcsin\zeta - \frac{\pi}{2}\right]\right\} \\ &\quad \text{for } \zeta_a \leqslant \zeta \leqslant 1, \end{aligned} \tag{20}$$

where $\zeta_a = a/L$. As will be discussed below, $\zeta_a$ is an important parameter for the SSDFT that represents largely the relative mechanical properties of the plate and die materials, and which influences the deformation of the plate significantly.

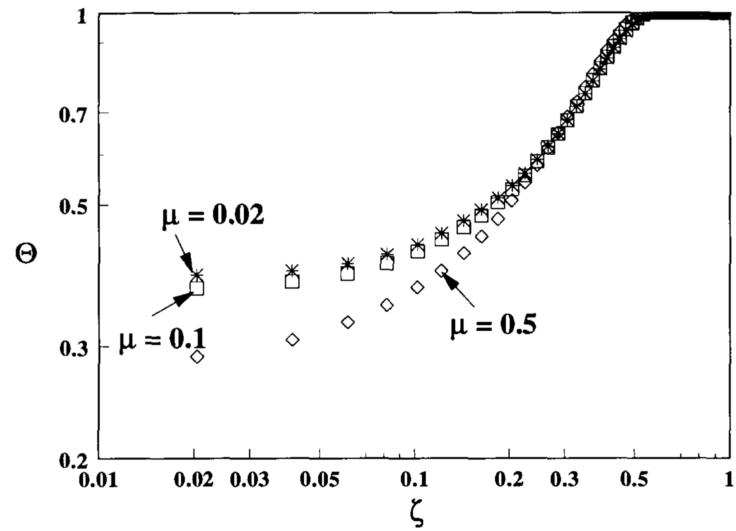


Fig. 7. Effect of $\mu$ on the spring–back ratio, for $\zeta_a = 0.8$ and $k = 1.5$.

A relevant study concerning the receding contact between a plate and an elastic foundation showed that the variation of $\zeta_a$ is non-linear even when the plate is elastic [3]. Nevertheless, when a approaches $h$, the value of $L$ will become constant [4], governed by the materials constants of the plate and foundation:

$$L = h\left(\frac{1.845E(1 - \nu_f^2)}{E_f(1 - \nu^2)}\right)^{1/3}, \tag{21}$$

where $E_f$ and $\nu_f$ are Young's modulus and Poisson's ratio of the foundation, respectively. Although the condition for obtaining Eq. (21) differs to a certain extent from the present stamping processes, it can be used to demonstrate qualitatively the importance of the ratio of $E$ to $E_f$ in a stamping process if the foundation is thought of as a die. It indicates that for a given plate material ($E$ given), a softer die (smaller $E_f$) will bring about a larger value of $L$ and vice versa.

The axial force in the plate is, according to Eq. (1),

$$n = \frac{a\mu\bar{p}^U}{2\sigma_Y h}\left(\frac{\pi}{2} - \arcsin\zeta - \zeta\sqrt{1 - \zeta^2}\right) + \frac{kL^2}{Ebh^2}\eta_c, \tag{22}$$

where $\mu$ has been assumed to be independent of $x$ and the central deflection of the plate, $w_c$ (its dimensionless quantity is $\eta_c$), is considered to be much smaller than $L$.

The dependence of the spring–back ratio upon parameters $k$, $\zeta_a$ and $\mu$ are presented in Figs. 7–9 within the idealisation of the present modelling (in all cases $\xi = 1.05$, $e = 0.2$, $\sigma_Y/E = 1/3$, $h/L = 0.1$ and $b = 1$). Generally, increasing $k$ and $\mu$ decreases the spring–back ratio and hence indicates that both axial tension and interface friction between the plate and die are principal factors in the reduction of $\Theta$. It is easy to see,

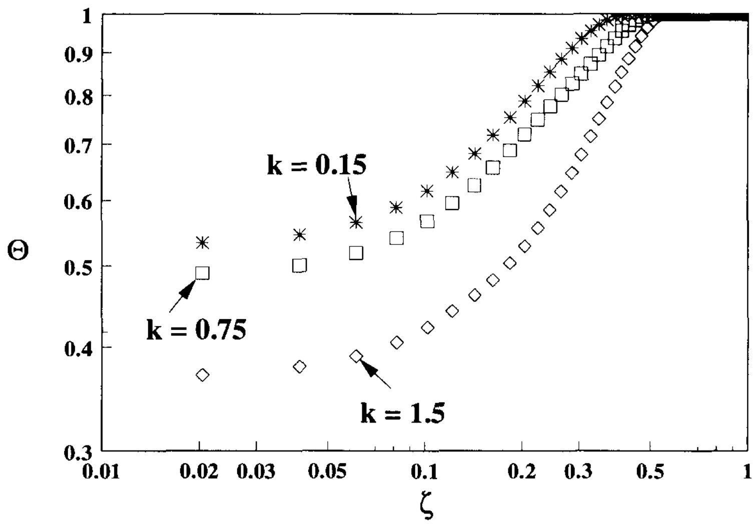


Fig. 8. Effect of $k$ on the spring-back ratio, for $\zeta_a = 0.8$ and $\mu = 0.1$.

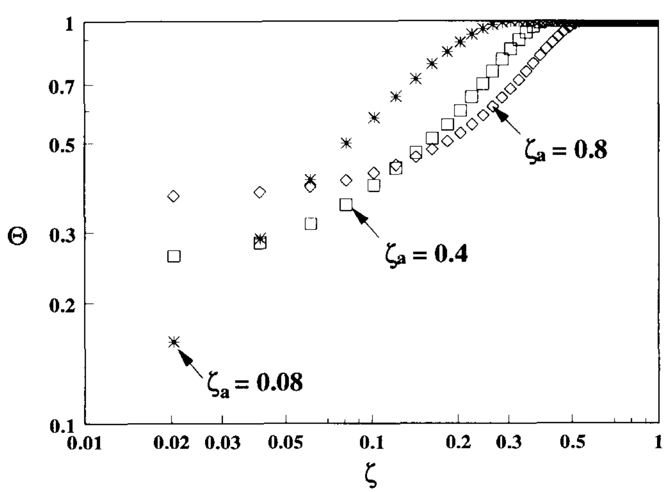


Fig. 9. Effect of $\zeta_a$ on the spring-back ratio, for $k = 1.5$ and $\mu = 0.1$.

however, that the contribution of $\mu$ is more localised under the assumption that $q^L(x)$ is proportional to $p^L(x)$ and that $\mu$ itself is independent of $x$. Furthermore, in the case of zero external tension, dies with higher friction properties would be better for the shape maintaining of workpieces after unloading.

Now consider the effect of $\zeta_a$ in Fig. 9. As have been discussed, a larger value of $\zeta_a$ could be considered as a stamping associated with a harder die (and vice versa) where

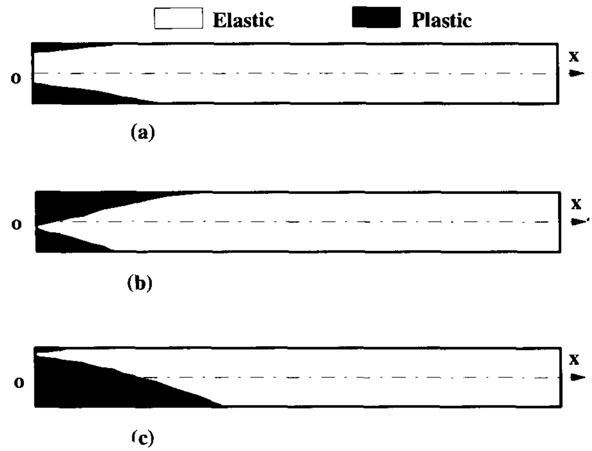


Fig. 10. Development of plastic zones for $\zeta_a = 0.8$, $\mu = 0.5$ and: (a) $\eta_c = 0.7$, $k = 1.5$; (b) $\eta_c = 1.2$, $k = 0.5$; and (c) $\eta_c = 1.2$, $k = 1.5$.

according to the results shown in Fig. 9, this causes larger spring–back ratio. However, if the die is too soft, as is the case of $\zeta_a = 0.08$, the residual curvature of the plate will be very non-uniform which is usually not desirable in practical stamping. Hence, the selection of the die material should be made carefully by considering the particular shaping requirement of individual stamping processes.

The inherent mechanism of the variation of $\Theta$ with the change of $k$, $\mu$ and $\zeta_a$ is indeed due to the change of the deformation mechanism of the plate, as shown in Fig. 10. With constant values of $k$, $\mu$ and $\zeta_a$, the upper compressive plastic zone shrinks when the punch displacement increases (represented by the increase of $\eta_c$ here, see Figs. 10(a) and (c)). Tensile plastic deformation is dominant in this case. When $k$ decreases, however, the compressive plastic deformation becomes considerable, which is why the value of $\Theta$ is remarkable for smaller values of $k$ (Fig. 8).

A comparison of the present results with those of conventional stamping by rigid dies can also be made. An obvious difference is that a SSDFT leads to workpieces with a much smoother distribution of curvature, which is not difficult to understand if the distinct loading stages (blank bending and ironing) and their corresponding deformation mechanisms in the conventional processes [1] are recalled. During blank bending, the contact between the plate and the punch surface is not continuous, caused by many localised curvature peaks. These peaks are usually very difficult to be ironed out in the following ironing stage. In a SSDFT, however, there is no blank bending, the deformable die always trying to make the plate match the punch surface through the interaction force $p^L(x)$.

Results representing real stamping processes can be obtained by using a realistic distribution of interface forces determined by the theory of contact mechanics or by experimental measurement.

## 5. Conclusions

A mechanics model has been proposed to study the plate stamping process by deformable dies subjected to plane-strain conditions. There are six possible stress states for any plate section, depending on the combination of axial force and bending moment. It has been found that the spring–back ratio is affected strongly by the properties of the deformable die for a given plate material. The friction properties and the relative magnitude of the elastic constants of the dies are the key parameters in process design. All of these can be interpreted by the detailed analysis of the development of the plastic zone in the plate.

## Acknowledgement

This work is supported by an ARC Small Grant.

## References

[1] T.X. Yu and L.C. Zhang, *Plastic Bending: Theory and Applications*, Science Press, Beijing, 1992.
[2] T.X. Yu and W. Johnson, Influence of axial force on the elastic-plastic bending and springback of a beam, *J. Mech. Work. Tech.*, 6 (1982) 5.
[3] M. Ratwani and F. Erdogan, On the plane contact problem for a frictionless elastic layer, *Int. J. Solids Structs*, 43 (1973) 921.
[4] G.M.L. Gladwell, On some unbounded contact problems in plane elasticity theory, *Trans. ASME, J. Appl. Mech.*, 43 (1976) 263.